Full Paper

Electrochemical Behavior and Voltammetric Determination of Quercetin in Foods by Graphene Nanosheets Modified Electrode

Mohammad Saber-Tehrani[1,*], Akram Pourhabib[1], Seyed Waqif Husain[1] and Majid Arvand[2]

[1]*Department of Chemistry, Science and Research Branch, Islamic Azad University, P.O. Box: 1415-775, Tehran, Iran*

[2]*Department of Chemistry, Faculty of Science, University of Guilan, Namjoo Street, P.O. Box: 1914, Rasht, Iran*

[*]Corresponding Author, Tel: +982144865777, Fax: +982144865777

E-Mail: drmsabertehrani@yahoo.com

Abstract- Quercetin belongs to the flavonol family. It is most abundant among the flavonoid molecules. A method was developed for quantification of quercetin in apple and onion using differential pulse voltammetry at graphene nanosheets modified glassy carbon electrode (GNs/GCE) and UV spectrophotometry as reference method. Interest graphene centers on its excellent mechanical, electrical, thermal and optical properties, it's very high specific surface area, and our ability to influence these properties through chemical functionalization. The electrochemical behavior of quercetin at the GNs/GCE was investigated, and the results indicated that the electrode reaction was controlled by adsorption. The anodic peak current almost stops increasing after 260 s accumulation. This indicates that the accumulation of quercetin at the electrode surface nearly reaches a saturation state after 260 s. The accumulation potential was analyzed between -0.6 and 0.3 V, a maximum peak was achieved at 0.2 V. Under the optimal conditions, the peak currents of DPV increased linearly with the quercetin concentration in the range from 0.006 to 10 µM and 10 to 100 µM with limit of detection 3.9 nM. The proposed method was successfully applied in the detection of quercetin in foods.

1. INTRODUCTION

Flavonoids are a group of polyphenolic compounds widely distributed the medicinal plant, vegetable, fruit juice and variety of beverages. Flavonoids have attracted an increasing interest in electrochemical sensing which are benzo-γ-pyrone derivatives with several hydroxyl group attached to the ring structures C_6-C_3-C_6; of which some contain *o*-dihydroxy catechol (the B ring) such as quercetin, rutin, catechin and luteolin, etc. [1]. Quercetin (3,3′,4′,5,7-penta hydroxyl flavones) is a flavonoid of widespread occurrence in plants (caper, lovage, broccoli, lettuce, spinach) and food of plant origin (onions, apples, various berries, tea) [2]. There is considerable evidence to show that a greater intake of apple contributes to improved health by reducing the risk of disease and some forms of cancer. Apple fruit is a major source of phenol compounds, because its consumption is widespread in many countries and it is available on the market for the whole year [3]. Onion (*Allium cepa* L.) is one of the most important vegetables worldwide with an estimated annual production of almost 47 million in year 2000. The main production areas are China, India, United States, Russia, Turkey, and Iran. Consumption per capita differs greatly between countries and areas, but a major trend seems to be that onion consumption increasing worldwide [4] Onions ranked highest in quercetin content in a survey of 28 vegetables and nine fruits [5]. The amount of quercetin in onions varies depending on bulb colour and type, being distributed mostly in the outer skin and rings [6]. The many studies have revealed various beneficial effects on human health, including anti-viral, anti-cancer, anti-inflammatory, and anti-tumor activity, and can protect human DNA from oxidative attack in vitro [7].

Up to now, methods for investigation of quercetin include spectrophotometry [8], gas chromatography combined with mass spectrometry [9], high performance liquid chromatography with UV detection [10], or spectrophotometric and coulometric detection [11]. These determination methods often require some complicated and time consuming pretreatments and/or expensive experimental equipments, so some electrochemical methods have been used for the determination of quercetin [7,12]. Several reports have been published for the electrochemical study of quercetin. Zielinska and Pierozynski investigated electro-oxidation of quercetin at glassy carbon electrode studied by a.c. impedance spectroscopy [2]. Xiao *et al.* studied voltammetric determination of quercetin at a multi-walled carbon nanotubes (MWCNTs) paste electrode [7]. Kim and Xu informed about the stable, reproducible and sensitive quantification of quercetin at pH 3.8 using a glassy carbon electrode (GCE) modified with CNTs dispersed in Nafion [12]. Jin *et al.* investigated the electrochemical characterization of a glassy carbon electrode modified with microbial succinoglycan monomers and multi-walled carbon nanotubes for the detection of quercetin in an aqueous electrolyte [13]. Lin *et al.* explored a direct simultaneous determination method for quercetin and rutin by using reversing differential pulse voltammetry at the MWCNTs

paste electrode [14]. Zare *et al.* studied the electrochemical mechanism of quercetin by using cyclic voltammetry, chronoamperometry and rotating disk electrode [15].

Graphene (GR), monolayer graphite, has attracted an increasing attention in recent years since its discovery in 2004 by Geim and co-workers [16]. GR is an exciting material. It has a large theoretical specific surface area (2630 m^2 g^{-1}), high intrinsic mobility (200 000 cm^2 V^{-1} s^{-1}) [17], high Young's modulus (~1.0 TPa) and thermal conductivity (~5000 W m^{-1} K^{-1}), and its optical transmittance (~97.7%) and good electrical conductivity merit attention for application such as for transparent conductive electrodes, among many other potential applications [18]. In comparison with CNTs, two advantages of graphene are apparent, as follows:

(1) Graphene does not contain metallic impurities as CNTs do [19]

(2) Graphite, which is used in production of graphene, is cheap and accessible

Graphene has great promise in electrochemical sensing and biosensing because of its superior electron conductivity and single-atom thickness [20]. It has been reported that graphene could be used as a very excellent electrocatalytic material towards the detection of variety of electro-active species, such as glucose [21,22], dopamine [23], H_2O_2 [24], DNA base [25], 4-aminophenol [26], catechol and hydroquinone [27] and paracetamol [28]. It has been shown that graphene and graphene-based materials are promising supplements or replacements for conventional carbon materials, such as carbon nanotubes and graphite. Even superior performance of graphene-based electrochemical sensors compared to carbon nanotubes has been reported, which is attributed to the presence of more sp^2-like planes and edge defect in graphene [29].

Current investigation presents a facile GNs-based approach for electrochemical detection of the quercetin. GNs were synthesized chemically by Staudenmaier procedure. The prepared GNs were characterized by TEM, FTIR and cyclic voltammetry (CV). The influence factors (such as acidity of the supporting electrolyte, scan rate, accumulation time and accumulation potential) for electrochemical determination of quercetin were given in this work.

2. EXPERIMENTAL SECTION

2.1. Reagents and solutions

Quercetin dihydrate was obtained from Alfa Aesar (Ward Hill, MA). Hydrazine hydrate (80%), ethanol, potassium chlorate and graphite powder (99.999% purity, −200 meshes) were purchased from Merck (Darmstadt, Germany). Aqueous solutions were prepared with phosphate buffer solution 0.1 M (pH 5.5). The stock solution of quercetin (0.4 mM) in phosphate buffer and ethanol mixture (85:15 v/v) was prepared daily and just before use. Double distilled water was used for the preparation of all solutions.

2.2. Apparatus

Electrochemical measurements were conducted using Autolab PGSTAT 30 electrochemical analyzer (Ecochemie BV, Utrecht, the Netherlands) connected to a computer with GPES (General Purpose Electrochemical System) software package. All electrochemical studies were performed at 25±1°C. A conventional three-electrode cell was employed incorporating a working modified electrode (GNs/GCE), a saturated Ag/AgCl reference electrode, and a platinum wire counter electrode. All potentials were measured and reported *vs.* Ag/AgCl reference electrode. Differential pulse voltammetric (DPV) experiments were performed using the pulse amplitude of 0.025 V s^{-1}, pulse interval time of 0.5 s and scan rate of 0.01 V s^{-1} over the potential range of 0.22–0.5 V *vs.* Ag/AgCl. UV measurements were carried out at room temperature by means of a Shimadzu UV-2100 spectrophotometer. The pH of the solutions was adjusted by a model 827 pH Lab Metrohm Swiss made. A model CM10 transmission electron microscope (TEM; Philips) and Fourier Transform Infrared (FT-IR) Shimadzu 8900 were used to characterize the morphology and size of the nanoscale graphene and to prove the reduction of graphene oxide to graphene, respectively. Freeze-drier (ALPHR 1-2 LD, Martin Christ Gefriertrocknungsanlagen GmbH, Germany) was used for drying the samples.

2.3. Synthesis of GNs

Graphene oxide was synthesized from graphite powder via Staudenmaier procedure. In brief, 5.0 g of expanded graphite was added in five portions to a stirred mixture of concentrated H_2SO_4 (87.5 mL) and fuming HNO_3 (45 mL) while cooling in an ice-water bath. To the mixture was added $KClO_3$ (55 g) in five separate portions for a period of 15 min with sufficient venting using nitrogen gas to reduce the risk of explosion upon generation of chlorine dioxide gas. The resulting slurry was stirred at room temperature for 96 h. The green slurry was poured into 4 L of ice water, and the mixture was filtered and subsequently washed with 5 L of 5% HCl. The filtered cake was then rinsed thoroughly with water until the filtrate was neutral. This was followed by rinsing the filter cake with methanol and diethyl ether, yielding 3.3 g of a fine brown powder of graphene oxide. The prepared graphene oxide was sonicated by a bath type sonicator (Sonoswiss SW3-H, 38 kHz, Switzerland) for 1 h at a power level of 240 W. After ultrasonication, samples were immediately precipitated by a centrifuge at 15000 rpm for 10 minutes. The graphene oxide sheets were extracted carefully. To get GNs, chemical reduction of the suspension of graphene oxide was carried out with 80% hydrazine hydrate (1.66 mL) at 80 °C for 24 h. Finally, black powder of GNs were obtained by filtration of the product and drying in vacuum [30].

2.4. Preparation of GNs/GCE and effective electrode area

The synthesized graphene nanosheets were dissolved in 10 mL N,N-dimethylformamide (DMF) with the aid of ultrasonic agitation for 1 h, resulting in a uniform black solution. Prior to modification, the glassy carbon electrode (GCE) was polished with 0.3 μm α-alumina slurry to mirror like surface, and then washed with 1:1 double distilled water and ethanol in an ultrasonic bath and dried in room temperature. The GNs/GCE was prepared by casting 10 μL of GNs-DMF suspension on the surface of cleaned GCE and dried naturally. Before using, the modified electrode (GNs/GCE) was carefully rinsed with double distilled water to remove the loosely attached GNs at the electrode surface.

The effective surface areas of bare GCE and GNs/GCE were obtained by cyclic voltammetry with 5 mM $K_3[Fe(CN)_6]$ as a probe at different scan rates. For a reversible process, the equation $I_p=(2.69\times10^5)n^{3/2}AD^{1/2}Cv^{1/2}$ is applied [31], where I_p refers to the peak current and A is the electrode area (cm^2). Herein, for 5 mM $K_3[Fe(CN)_6]$, $n=1$, $D=7.6\times10^{-6}$ cm^2 s^{-1} (0.1 M KCl), C is the concentration of $K_3[Fe(CN)_6]$, v is the scan rate. The effective surface areas of the GCE and GNs/GCE were computed to be 0.038 and 0.075 cm^2, respectively. The GNs/GCE effective surface area is closely 2 times larger than that of the bare GCE, showing that the bare electrode was modified efficiently by GNs.

2.5. Real Samples

2.5.1. Preparation of onion

Two onion white and yellow (originated from Zanjan, Iran) were purchased from retail markets, and it was cut into small pieces and dried in a dry oven for 24 h. 4.0 g of dried onion was then taken and homogenized. The homogenates were extracted with ethanol while stirring for 24 h in the absence of light at room temperature. The extracted material was filtered through Whatman filter paper under vacuum. After the filtrate was recovered, ethanol was evaporated at 80 °C until ca. 90% of the filtrate was evaporated. The prepared sample was then diluted to 50 mL with ethanol and filtered through 0.45 μm cellulose membranes [12]. The onion extract was stored in a refrigerator for further use.

2.5.2. Preparation of apple

Two apple varieties, namely green apple and golden apple (originated from Isfahan, Iran) were purchased from local grocery stores. Apple was mechanically peeled. Apple peel was frozen in liquid nitrogen and freeze-dried. Then, the dried peel was crush in closed vial to avoid hydration, obtaining a homogenous powder that was stored at room temperature in desiccator until analysis. Freeze-dried apple peel powder (0.5 g) was extracted with 30 mL of methanol-water-acetic acid (30:69:1, v/v/v) in ultrasonic bath during 10 min. Afterwards, the extract was freeze-dried once methanol had been evaporated at 40°C in a rotavapor (Laborata 4000; Heidolph Instruments GmbH&Co. KG, Germany) [32]. Then 0.2 g of the extract

dissolved in 15 mL ethanol in the absence of light at room temperature. A filtered 10 mL aliquot of sample was diluted to 100 mL with the phosphate buffer and the pH adjusted to 5.5. The prepared solution (25 mL) was transferred into the electrochemical cell. The standard addition method was used for quantification and the quercetin content of the aqueous extract of apple samples was determined.

3. RESULTS AND DISCUSSION

3.1. Characterization of synthesized GNs

Fig. 1A shows the morphology of GNs by TEM. The achieved TEM image showed a few layered structures for the GNs, and the transparent sheets are flake-like with wrinkles.

FT-IR spectra were used to investigate graphene oxide and GNs (Fig. 1B). In the FT-IR spectrum of graphene oxide (Fig. 1B(a)), the bands around 3434, 1718, 1361, 1242, 1132 and 1028 cm^{-1} are attributed to the oxygen-containing functional groups on graphene oxide [33], confirming the successful oxidation of graphite. After the reduction, only residual oxygen functionalities with much reduced intensity are present on the GNs surface as shown in Fig. 1B(b), suggesting the considerable deoxygenation by the chemical reduction process with hydrazine hydrate.
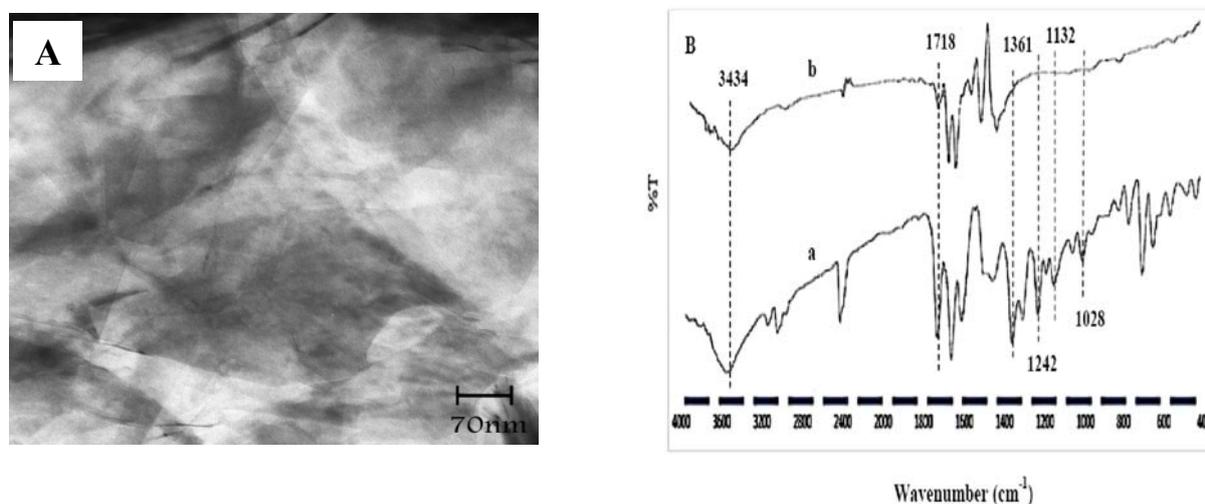

Fig. 1. (A) TEM image of graphene nanosheet. (B) FTIR spectrum of (a) graphene oxide and (b) graphene nanosheet

3.2. Electrochemical behavior of quercetin at the GNs/GCE

Fig. 2 shows the cyclic voltammograms of GNs/GCE in the absence of quercetin just in 0.1 M phosphate buffer and ethanol mixture (85:15 v/v) (Fig. 2a), bare GCE (Fig. 2b) and

GNs/GCE (Fig. 2c) in presence of 50 μM quercetin in 0.1 M phosphate buffer and ethanol mixture (85:15 v/v) (pH 5.5). At bare GCE, quercetin is reversibly oxidized with a formal potential at 0.36 V (Fig. 2b). This redox peak has been known as two-electron and two-proton process of the catechol moiety, 3′,4′-dihydroxyl group at ring B to ketone group. Further scan to positive potential displayed additional oxidation peak whose nature are known as the oxidation of other hydroxyl groups but are not of interest in this research. In the presence of 50 μM quercetin at GNs/GCE, a couple of redox peaks can be achieved with separation (ΔE_p) close to 0.081 V. Although no obvious difference in peak potential of quercetin can be observed at GCE and GNs/GCE, the redox peak current at GNs/GCE was 13.8 μA, which was almost 6-fold larger than at bare GCE (2.27 μA). Thus GNs must have a great effect on the kinetics of electrode reaction for the quercetin and must provide a suitable environment for the quercetin to transfer electrons with underlying GC electrode. The reason for the better performance of the GNs/GCE is not only attributable to the increment of electrode surface area, but also attributable to the more feasible electron transfer between quercetin and GNs through π-π interaction since quercetin has catechol moiety.
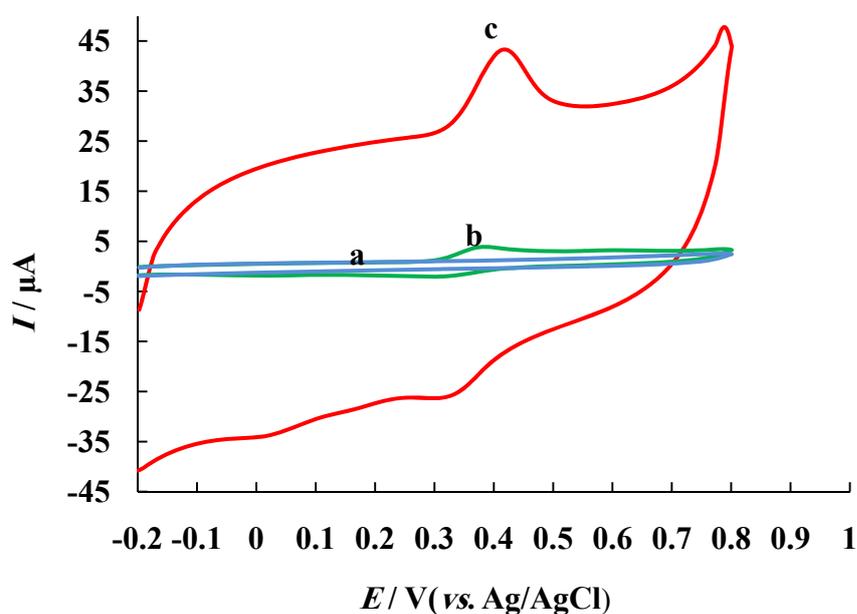

Fig. 2. Cyclic voltammograms (a) GNs/GCE in the absence of quercetin just in 0.1 M phosphate buffer and ethanol mixture (85:15 v/v), (b) bare GCE and (c) GNs/GCE in presence of 50 μM quercetin in 0.1 M phosphate buffer and ethanol mixture (85:15 v/v) (pH 5.5)

3.3. Effect of pH

The electrochemical behavior of quercetin is strongly depended on solution pH. To achieve an optimal electrochemical response of quercetin at GNs/GCE, the effect of pH was investigated by CV in the range of 2.1–7.2. As can be seen in inset B of Fig. 3, the redox peak current increased with solution pH ranging from 2.1 to 5.5, and then the decrease of the redox peak current was observed when the solution pH was higher than 5.5. When the pH exceeds 8, the anodic peak current disappears. The pH value of 5.5 was chosen as the optimal pH condition and utilized in the subsequent experiments. The peak potentials were also related to the solution pH. Cyclic voltammetry was carried out to characterize the effects of solution pH on redox peak potentials of quercetin on GNs/GCE at a scan rate of 100 mV s^{-1}. The values of oxidation peak potential shifted to more negative potentials with the increase of pH (Fig. 3, inset A) indicating that protons take part in the electrode reaction process. The linear regression equation of quercetin is thus achieved $E_{pa}(V)=0.636–0.0581pH$ with a correlation coefficient of 0.9851. The slope of d_{Ep}/d_{pH} of plot is close to 59 mV/pH, indicating that the electrode process is an equal proton-electron transfer, which is in accordance with previous reports [7,12,15]. The possible electrochemical redox reaction mechanism of quercetin can be expressed as shown in Scheme 1.
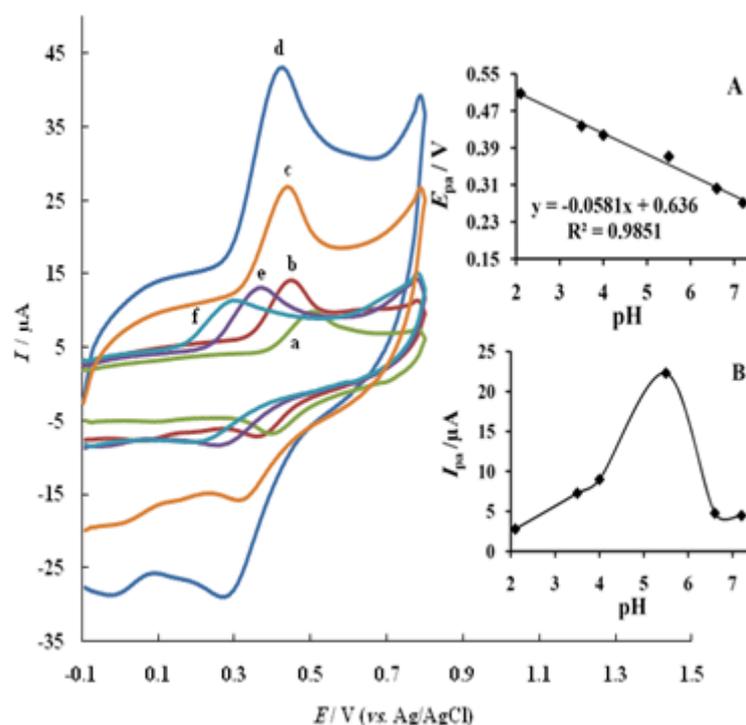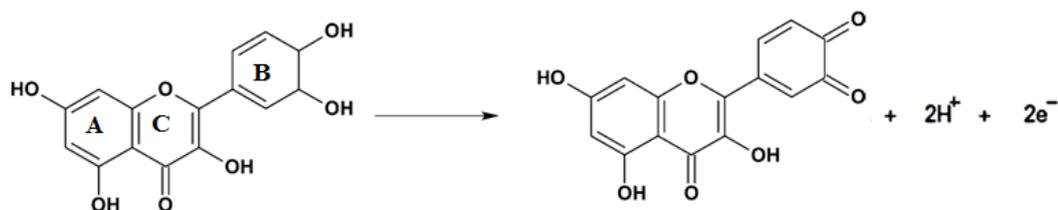

Fig. 3. Cyclic voltammograms for GNs/GCE in 0.1 mol L^{-1} phosphate buffer containing 50 µmol L^{-1} quercetin at different pHs: (a) 2.1, (b) 3.5, (c) 4, (d) 5.5, (e) 6.6 and (f) 7.2. Inset A: The linear relationship of the anodic peak potential *vs.* pH. Inset B: The linear relationship of the anodic peak current *vs.* pH

Scheme 1. The redox reaction mechanism of quercetin

3.4. Effect of scan rate

The effect of the scan rate on the peak current of 50 μM quercetin was investigated in 0.1 M phosphate buffer and ethanol mixture (85:15 v/v) (pH 5.5) at GNs/GCE (from 20 to 200 mV s^{-1}). It is clear that both the redox peak currents enhanced with increasing the scan rate, indicating that the electrode reaction of quercetin is controlled by adsorption (Fig. 4A). The regression equation is I_{pa} (μA) = 0.339v (mV s^{-1})+4.786 (R^2=0.996) (Fig. 4A, inset). With the increase of scan rate the peak-to-peak separation (ΔE_p) also increased gradually, so the electrochemical parameters of the electrode reaction were calculated according to the Laviron's equations [34]:

$$E_{pa} = E^{o'} + \frac{2.303RT}{(1-\alpha)nF}\log v + \frac{2.303RT}{(1-\alpha)nF}\log\frac{nF(1-\alpha)}{RTk_s} \qquad (1)$$

$$E_{pc} = E^{o'} - \frac{2.303RT}{\alpha nF}\log v - \frac{2.303RT}{\alpha nF}\log\frac{\alpha nF}{RTk_s} \qquad (2)$$

$$\log k_s = \alpha\log(1-\alpha) + (1-\alpha)\log\alpha - \log\frac{2.303RT}{nFv} - \frac{\alpha(1-\alpha)nF\Delta E_p}{2.3RT} \qquad (3)$$

where α is the charge transfer coefficient, n is the number of electrons transferred and k_s is the apparent heterogeneous electron transfer rate constant. Two straight lines were obtained with the equations as E_{pa} (V)=0.07log$v$+0.301 (R^2=0.991) and E_{pc} (V)=-–0.08log$v$+0.447 (R^2=0.993) (Fig. 4B). Then the values of α and k_s were calculated as 0.53 and 5.31×10^{-6} s^{-1}, respectively. The value of n was further calculated to be 1.84.
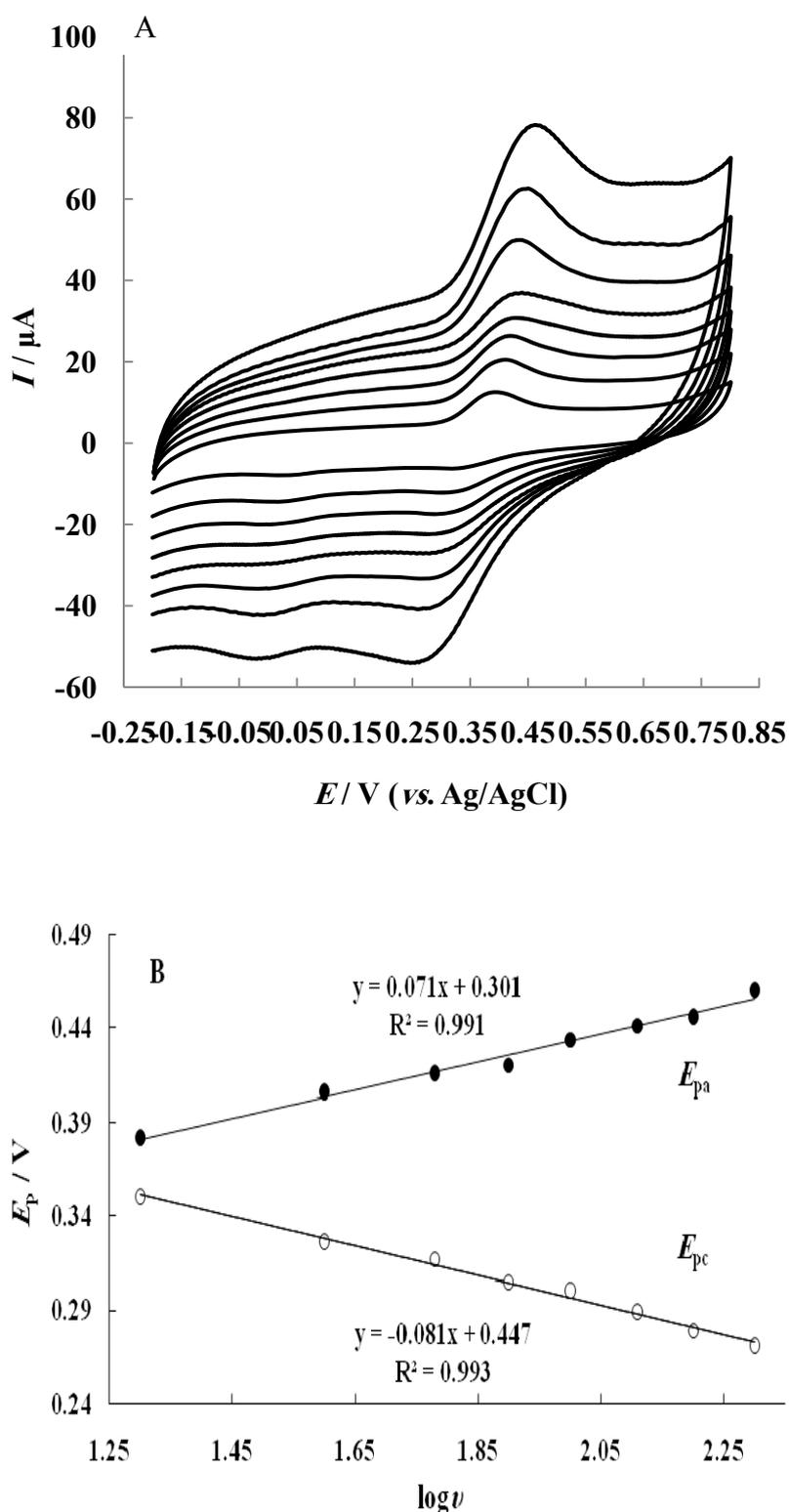
Fig. 4. (A) Cyclic voltammograms of 50 µM quercetin on the GNs/GCE at different scan rates in 0.1 M phosphate buffer (pH 5.5): (a), 20, 40, 60, 80, 100, 130, 160, and 200 mV s^{-1}. Inset: relationship between anodic peak current and potential scan rate for 50 µM quercetin on the GNs/GCE in 0.1 M phosphate buffer (pH 5.5)

3.5. Optimization of DPV parameters for quercetin analysis

The effect of accumulation potential and time on the anodic peak current response of quercetin was investigated by DPV. The anodic peak current almost stops increasing after 260 s accumulation (Fig. 5A). This indicates that the accumulation of quercetin at the electrode surface nearly reaches a saturation state after 260 s. The accumulation potential was analyzed between -0.6 and 0.3 V (Fig. 5B), a maximum peak was achieved at 0.2 V. Similar behavior has been previously reported for the electrochemical oxidation of quercetin on the surface of carbon nanotubes-paste electrode [7]. In this work 260 s was selected as the accumulation time and 0.2 V as the accumulation potential.
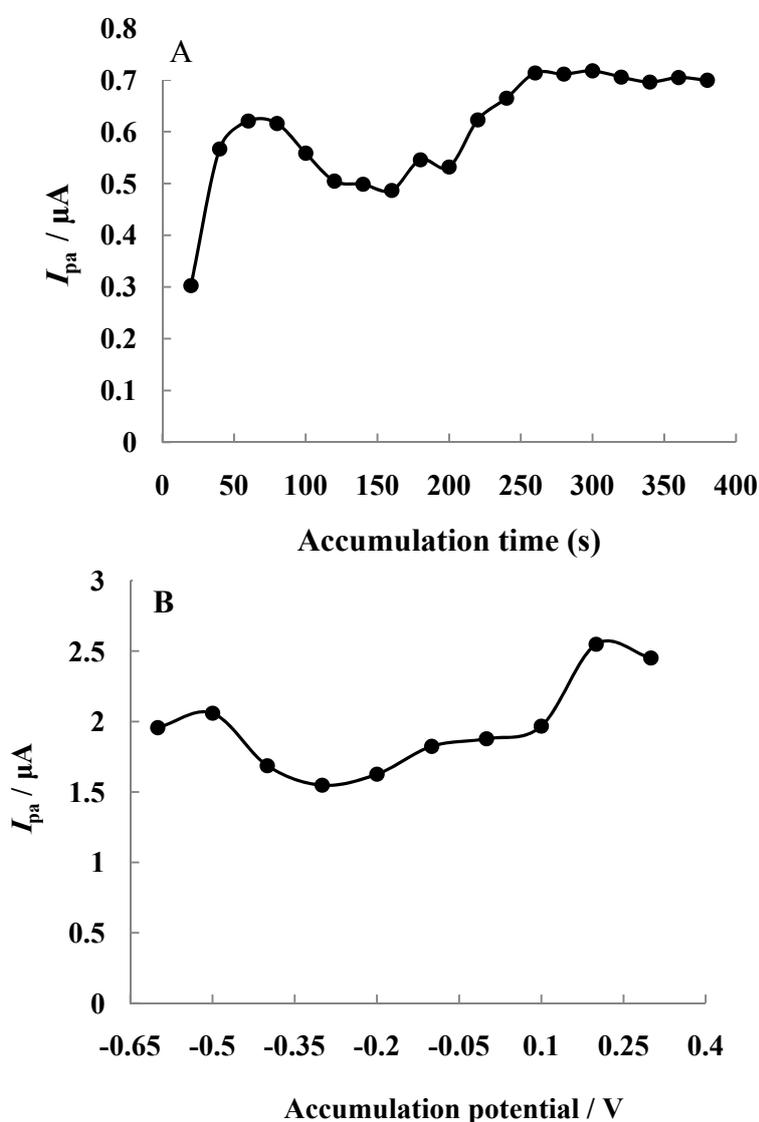

Fig. 5. Effect of accumulation time (A) and potential (B) on the anodic peak current of 1 μM quercetin in 0.1 M phosphate buffer (pH 5.5)

To know whether the quercetin adsorbs on the GNs/GCE surface or not, a simple experiment was carried out. The GNs/GCE was immersed into 50 μM quercetin solution for 60 s. Then it was taken out from the solution, thoroughly rinsed with pure water and put into the phosphate buffer solution (pH 5.5). After this process, the cyclic voltmmogram was recorded and is shown in Fig. 6. As can be seen, a similar voltammogram was obtained, with only decrease of peak current. By many times scanning, the redox peaks were disappeared. This experiment obviously illustrated that quercetin could be adsorbed onto the GNs/GCE electrode surface and the stability of adsorption of quercetin was not very good.
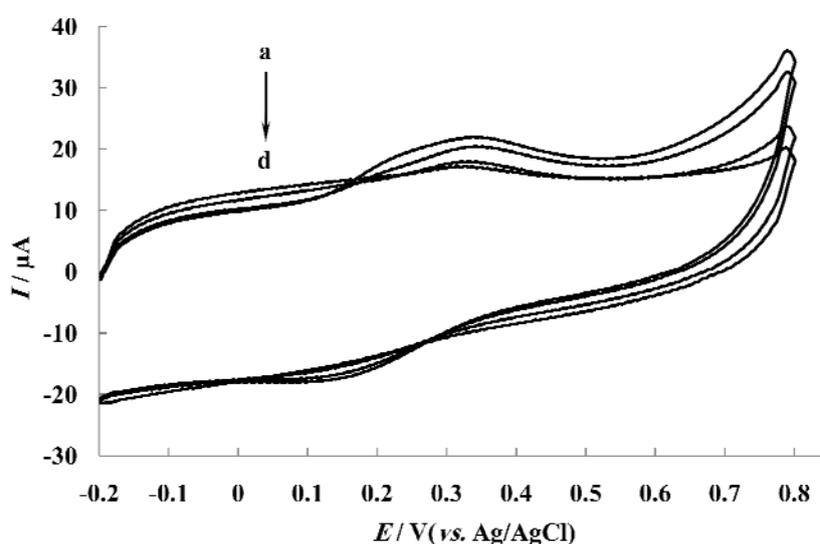

Fig. 6. Repetitive cyclic voltammograms of GNs/GCE taken out from 50 μM quercetin with 60 s accumulation time in phosphate buffer (pH 5.5) at difference cyclic number (a–d): 1, 10, 50, 100. Scan rate: 100 mV s^{-1}

3.6. Analytical performance

Differential pulse voltammetry was performed to investigate the relationship between the peak current and concentration of quercetin due to its higher sensitivity. Under the optimal conditions, when the concentration of quercetin changes from 0.001 to 400 μM, the anodic peak current and quercetin concentration show linear relationship in the ranges of 0.006 to 10 μM and 10 to 100 μM, respectively (Fig. 7). The regression equations are: I_{pa} (μA)=0.401C (μM)+0.209 (R^2=0.997) for the range of 0.006–10 μM and I_{pa} (μA)=0.057C (μM)+3.211 for the range of 10–100 μM (R^2=0.992). The slopes of the two calibration plots are different, which is related to the change of accumulation efficiently. The detection limit was then estimated to be 0.0039 μM (3.9 nM).
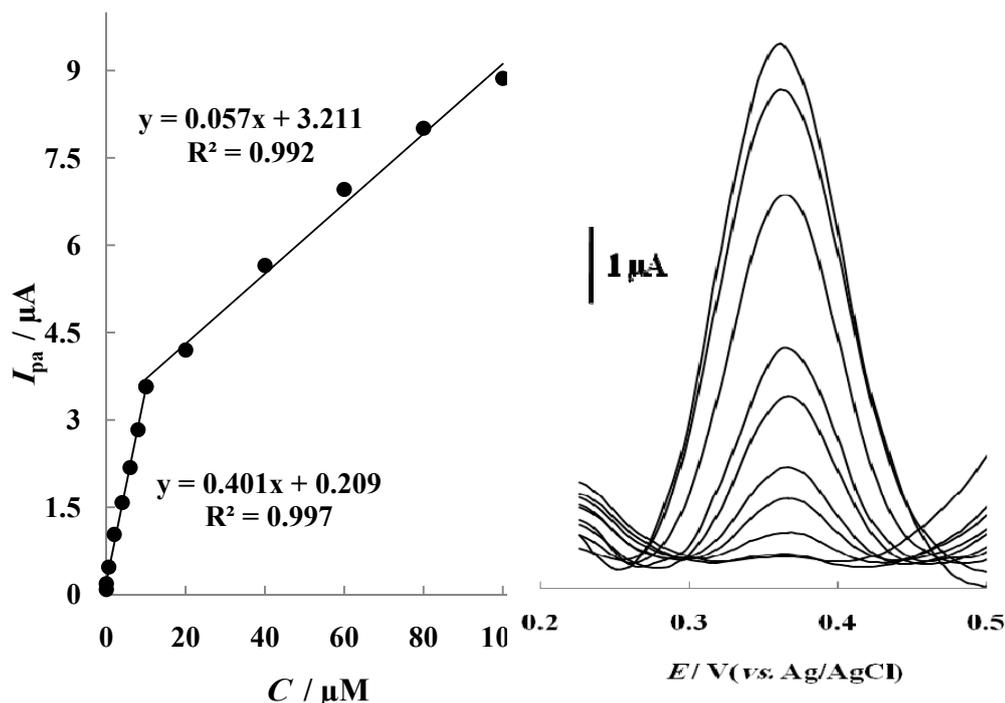
Fig. 7. Relationship of current responses to quercetin concentration. Inset: DPVs for GNs/GCE, with the optimized parameters. The quercetin concentrations are from 0.006–10 μM and 10–100 μM in 0.1 M phosphate buffer (pH 5.5)

To estimate the fabrication reproducibility of the GNs/GCE, the relative standard deviation (RSD%) of five electrodes prepared independently for measuring 1.0 μM quercetin was calculated to be 3.15%, indicating the good fabrication reproducibility. The measurement repeatability of the GNs/GCE was investigated with the same quercetin concentration. The RSD% was 2.8% for 8 repetitive assays. This result revealed that this method has good repeatability. A comparison of the proposed electrode with recently reported methods listed in Table 1 shows that GNs/GCE is superior to the existing electrodes.

3.7. Interference study

The influence of some organic compounds on the determination of quercetin was studied by DPV. The results indicated that 6-fold of ascorbic acid and methoxy phenol, 8-fold of uric acid and 10-fold of glucose did not interfere with the oxidation signal of 10 μM quercetin (peak current change <±10%).

Fig. 8 shows the differential pulse voltammograms of quercetin samples before (a) and after (b) addition of 20 μM uric acid. It can be seen that only one oxidation peak was observed in the absence of uric acid, which could be attributed to the oxidation of quercetin. When uric acid was added into quercetin sample, two oxidation peaks were achieved with the peak potential of 0.497 and 0.367 V for uric acid and quercetin, respectively. The peak-to-

peak separation of quercetin and uric acid was 0.13 V, which is enough for their simultaneous determination.

Table 1. Comparison of the responses of different quercetin sensors

Electrode	Modifier	Linear range (µM)	Detection limit (µM)	Real sample	Ref.
Glassy carbon	MWCNTs	0.002–0.1 and 0.1–20	–	–	[7]
Glassy carbon	MWCNTs and succinoglycan monomer	2.36–59	–	–	[13]
Glassy carbon	MWCNTs dispersed in polyethyleneimine	0.8–7.0	0.089	Onion	[35]
Glassy carbon	MWCNTs dispersed in polyacrylic acid	0.1–5.0	0.0075	Onion	[35]
Graphite disc electrode	MWCNTs and parafin	0.009–40	0.0048	–	[36]
Glassy carbon	Carbon nanotube and Nafion	0.02–6.3	–	Onion	[12]
Glassy carbon	Graphene nanosheets	0.006–10 and 10–100	0.0039	Apple, onion	This work

3.8. Determination of quercetin in real samples

To demonstrate the performance of the proposed electrode in real samples analysis, the content of quercetin in apple (golden, green) and onion (yellow, white) samples was measured by standard addition method at GNs/GCE by DPV. The accuracy of the proposed method was compared to the standard UV-Vis spectrophotometric method (Table 2). The UV-Vis spectrum of quercetin, like most flavones and flavonols, consists of two major absorption maxima, one of which occurs in the range 240–285 nm (band II belonging to A-ring benzoyl system) and the other in the range 300–400 nm (band I belonging to B-ring cinnamoyl system) [1]. The UV-Vis absorption spectra of green apple extract before and after adding of 0.5 µM quercetin in the 0.1 M phosphate buffer solution pH (5.5) were obtained (Fig. 9). The results demonstrate that the proposed voltammetric method using GNs/GCE is applicable and acceptable for determination of quercetin in food samples.
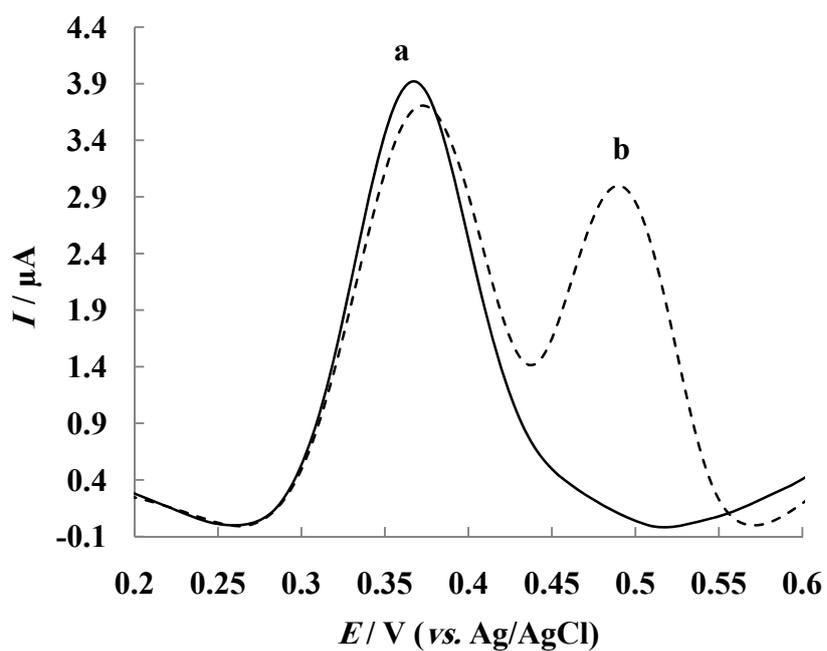
Fig. 8. The differential pulse voltammograms of quercetin before (a) and after (b) addition 20 µM uric acid
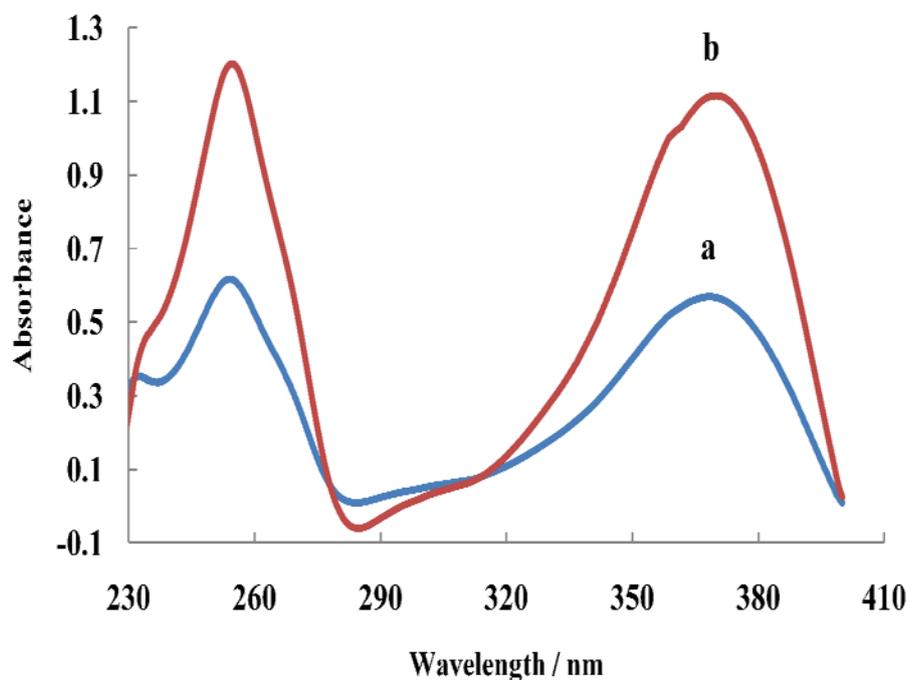

Fig. 9. UV-Vis absorption spectra of (a) green apple extract and (b) a + 0.5 µM quercetin in the 0.1 M phosphate buffer solution (pH 5.5)

Table 2. Results of the quercetin determination in foods by differential pulse voltammetry compared with spectrophotometric method (λ=365 nm)

Sample	Quercetin (mg Kg^{-1})[a]				t-test[b]	F-test
	Proposed method	RSD (%)	Reference method	RSD (%)		
Green apple	1.98±0.11	5.56	2.11±0.09	4.26	2.04	1.49
Golden apple	3.89±0.17	4.37	4.02±0.08	1.99	1.55	4.52
White onion	12.39±0.74	5.97	13.17±0.69	5.24	1.72	1.15
Yellow onion	28.76±1.53	5.32	30.04±1.19	3.96	1.48	1.65

[a]$x = \bar{x} \pm s_x$ for $n = 5$ and s_x denotes standard deviation
[b]The theoretical values of t and F at P= 0.05 are 2.31 and 6.39, respectively

4. CONCLUSIONS

In this paper, a simple and sensitive electrochemical method for quercetin determination based on graphene nanosheets modified glassy carbon electrode was developed. Owing to the unique properties of GNs, including π-π interaction, the high electron-transfer kinetics of the GNs/GCE, strong adsorptive ability and high density of edge-plane-like defective sites, the GNs modified electrode obviously promotes the sensitivity of the determination of quercetin. The proposed electrode exhibited a good performance in terms of sensitivity, detection limit, and repeatability. Under the optimized conditions, the anodic peak current is linear to quercetin concentration in the ranges of 0.006 to 10 μM and 10 to 100 μM with detection limit 3.9 nM. Electroanalytical determinations were much faster and cheaper than the chromatographic method, and there is an additional advantage of avoiding consume of a large amounts of toxic organic solvents such as methanol. Moreover, the proposed electrode can be applied to simultaneously determine uric acid and quercetin due to the enough peak-to-peak separation.

REFERENCES

[1]   Z. Wang, J. Xia, L. Zhu, X. Chen, F. Zhang, Sh. Yao, Y. Li, and Y. Xia, Electroanal. 23 (2011) 2463.
[2]   D. Zielinska, and B. Pierozynski, J. Electroanal. Chem. 625 (2009) 149.
[3]   A. Wojdylo, J. Oszmiański, and P. Laskowski, J. Agric. Food. Chem. 56 (2008) 6520.
[4]   R. Slimestad, T. Fossen, and I. M. Vagen, J. Agric. Food. Chem. 55 (2007) 10067.

[5]   M. G. L. Hertog, P. C. H. Hollman and M. B. Katan, J. Agric. Food Chem. 40 (1992) 2379.

[6]   D. Zielińska, L. J. Nagels, and M. K. Piskula, Anal. Chim. Acta 617 (2008) 22.

[7]   P. Xiao, F. Zhao, and B. Zeng, Michrochim. J. 85 (2007) 244.

[8]   Z. Nikolovska-Coleska, L. J. Klisarova, L. J. Suturkova, and K. Dorevski, Anal. Lett. 29 (1996) 97.

[9]   D. G. Watson, and E. J. Oliveira, J. Chromatogr. B 723 (1999) 203.

[10]   S. E. Nielsen, and L. O. Dragsted, J. Chromatogr. B 707 (1998) 81.

[11]   M. Careri, L. Elviri, A. Mangia, and M. Musci, J. Chromatogr. A 881 (2000) 449.

[12]   G. R. Xu, and S. Kim, Electroanal. 18 (2006) 1786.

[13]   J. H. Jin, C. Kwon, W. Park, S. Kim, and S. Jung, J. Electroanal. Chem. 623 (2008) 142.

[14]   X. Q. Lin, J. B. He, and Z. G. Zha, Sens. Actuators B 119 (2006) 608.

[15]   H. R. Zare, M. Namazian, and N. Nasirizadeh, J. Electroanal. Chem. 584 (2005) 77.

[16]   K. S. Novoselov, A. K. Geim, S. V. Morozov, D. Jiang, Y. Zhang, S. V. Dubonos, I. V. Grigorieva, and A. A. Firsov, Science 306 (2004) 666.

[17]   K. I. Bolotin, K. J. Sikes, Z. Jiang, M. Klima, G. Fudenberg, J. Hone, P. Kim, and H. L. Stromer, Solid States Commun. 146 (2008) 351.

[18]   Y. Zhu, S. Murali, W. Cai, X. Li, J. W. Suk, J. R. Potts, and R. S. Ruoff, Adv. Mat. 22 (2010) 3906.

[19]   M. Pumera, Chem. Eur. J. 15 (2009) 4970.

[20]   G. Zeng, Y. Xing, J. Gao, Z. Wang, and X. Zhang, Langmuir 26 (2010) 15022.

[21]   X. H. Kang, J. Wang, H. Wu, I. A. Aksay, J. Liu, and Y. H. Lin, Biosens. Bioelectron. 25 (2009) 901.

[22]   Q. Zeng, J. S. Cheng, X. F. Liu, H. T. Bai, and J. H. Jiang, Biosens. Bioelectron. 26 (2011) 3456.

[23]   Y. Wang, Y. Li, L. Tang, J. Lu, and J. Li, Electrochem. Commun. 11 (2009) 889.

[24]   K. Wang, Q. Liu, X. Y. Wu, Q. M. Guang, and H. N. Li, Talanta 82 (2010) 372.

[25]   Y. Bo, H. Yang, Y. Hu, T. Yao, and S. Huang, Electrochim. Acta 56 (2011) 2676.

[26]   H. Yin, Q. Ma, Y. Zhou, S. Ai, and L. Zhu, Electrochim. Acta 55 (2010) 7102.

[27]   H. Du, J. Ye, J. Zhang, X. Huang, and C. Yu, J. Electroanal. Chem. 650 (2011) 209.

[28]   X. Kang, J. Wang, H. Wu, J. Liu, I. A. Aksay, and Y. Lin, Talanta 812 (2010) 754.

[29]   X. Huang, Z. Yin, S. Wu, X. Qi, Q. He, Q. Zhang, Q. Yan, F. Boey, and H. Zhang, Small 7 (2011) 1876.

[30]   J. R. Lomeda, C. D. Doyle, D. V. Kosynkin, W. H. Hwang, and J. M. Tour, J. Am. Chem. Soc. 130 (2008) 16201.

[31]   S. Alwarappan, C. Liu, A. Kumar, and C. Z. Li, J. Phys. Chem. C 114 (2010) 12920.

[32]　R. M. Alonso-Salces, K. Ndjoko, E. F. Queiroz, J. R. Ioset, K. Hostettmann, L. A. Berrueta, B. Gallo, and F. Vicente, J. Chromatogr. A 1046 (2004) 89.

[33]　L. H. Tang, Y. Wang, Y. M. Li, H. B. Feng, J. Lu, and J. H. Li, Adv. Funct. Mater. 19 (2009) 2782.

[34]　E. Laviron, J. Electroanal. Chem. 101 (1979) 19.

[35]　F. Gutiérrez, G. Ortega, J. L. Cabrera, M. D. Rubianes, and G. A. Rivas, Electroanal. 22 (2010) 2650.

[36]　G. Jin, J. B. He, Z. B. Rui, and F. S. Meng, Electrochim. Acta 51 (2006) 4341.